

Stabilization of Silica Gel against Hydrolysis by Doping with F⁻ or Zr(IV)

Khaled S. Abou-El-Sherbini¹, Peter G. Weidler², Detlef Schiel³, Mohey H. A. Amr⁴,
Henning Niemann³, Shady El-Dafrawy⁵, Wolfgang H. Höll^{2*}

¹Department of Inorganic Chemistry, National Research Centre, Dokki, Egypt

²Institute of Functional Interfaces (IFG), Karlsruhe Institute of Technology (KIT), Campus Nord, Karlsruhe, Germany

³Anorganische Analytik, Labor 3.11, Physikalisch-Technische Bundesanstalt Braunschweig,
Braunschweig, Germany

⁴Research Department, Trace Elements Lab, Chemistry Administration, Cairo, Egypt

⁵Department of Chemistry, Faculty of Science, Mansoura University, Mansoura, Egypt

Email: kh_sherbini@yahoo.com, peter.weidler@kit.edu, Detlef.Schiel@ptb.de, Henning.Niemann@ptb.de

Received October 17, 2013; revised November 17, 2013; accepted November 24, 2013

Copyright © 2014 Khaled S. Abou-El-Sherbini *et al.* This is an open access article distributed under the Creative Commons Attribution License, which permits unrestricted use, distribution, and reproduction in any medium, provided the original work is properly cited. In accordance of the Creative Commons Attribution License all Copyrights © 2014 are reserved for SCIRP and the owner of the intellectual property Khaled S. Abou-El-Sherbini *et al.* All Copyright © 2014 are guarded by law and by SCIRP as a guardian.

ABSTRACT

Silica gel (SG) was synthesized via acidification of sodium silicate solution then doped with F⁻ or Zr(IV) in molar ratios of F/Si 3/100, and Zr/Si 0.75/100 and 3.75/100 and sintered at 500°C, 800°C and 1000°C. The samples were investigated by X-ray diffractometry, infrared absorption and Raman spectra, surface area measurement, and inductively coupled plasma-optical emission spectrometry-monitored silica hydrolysis. All samples are mesoporous with BET surface areas 181.5 - 523.9 m²·g⁻¹. The surface area of the silica samples decreases as the sintering temperature increases. The hydrolysis process of silica decreases as the sintering temperature increases and as the surface area decreases. The pH and the type of buffer solution affect the hydrolysis of silica samples due to a SN₂ reaction mechanism favored in basic media using ammonia buffer. Zr(IV) increases the stability of silica samples against the hydrolysis as confirmed by the structural investigation, surface area and silica hydrolysis. F⁻ observably decreases the silica hydrolysis process when presenting on the surface of SG.

KEYWORDS

Silica Gel; Doping; Hydrolysis; Fluorine; Zirconium

1. Introduction

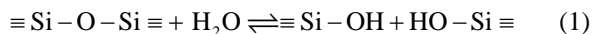
Silica is a polysiloxane polymer in which SiO₄ tetrahedra are arranged in a three-dimensional network producing many crystalline and amorphous structures. The amorphous silica, in particular, is practically inert to many media, wettable and has known chemical properties. Finally, it can be synthesized from cheap natural feedstocks and is not an environmental hazard [1,2]. Silica Gel (SG), is one of the most important amorphous forms of silica that can be synthesized with surface areas up to 1300 m²·g⁻¹, while maintaining good mechanical stability. These characteristics best meet the requirements of ideal support for many heterogeneous advanced applications

such as artificial bone implantaion [3,4], catalysis [5-7], sensors [8-10], fuel cells [11-13], and solid phase extraction [14-22].

Despite the importance of SG as a supporting material, its main disadvantage is the hydrolysis in hydro-systems. In aqueous media, the silica hydrolysis slightly occurs in weak acidic solutions and increases as the pH increases [19]. This is explained as, at the silica surface, the bulk structure terminates in either siloxane group (≡Si-O-Si≡) with the oxygen atom on the surface, or one of the several forms of silanol groups (isolated, vicinal or geminal 4 - 5 group/nm²) [1,19-22]. Under basic conditions, the silicon centers readily undergo nucleophilic attack by hydroxide ions in a topochemical reaction that results in addition of water to the siloxane bond *i.e.*, the siloxane

*Prof. Dr. W. Höll is deceased.

bonds are broken and replaced by silanol bonds according to Equation (1).



For highly alkaline solutions, the principal solute species is the monomer $\text{H}_2\text{SiO}_4^{2-}$ [23]. The aforementioned studies illuminate further aspects of silica hydrolysis; surface area, including temperature, bacteria, inhibitory-catalytic ion effects, aqueous transport, or the degree of disequilibrium [1,2,19-22]. For example, the silica hydrolysis either increases in the presence of amine-containing compounds as a functionalization group directly bonded via Si-C bond such as the 3-aminopropyl group [19-21] or freely presents in the aqueous medium such as ammonium ions [20]. This is attributed to the local basicity of the free amino group, which catalyzes the hydrolysis of siloxane bonds in the presence of water. Zhmud *et al.* [24-26] concluded from OH stretching vibrations that the aminopropyl chain participates in the formation of hydrogen bonds between amino groups and residual silanols on the surface of dry AP-SG. In the presence of water, this interaction can partly promote proton transfer from silanols to amino groups, which lead to the formation of Zwitter-ion-like moieties (e.g., $\equiv \text{SiO}^-$, $^+\text{H}_3\text{N}-$) on the silica surface [25,26].

The general base-catalyzed mechanism suggest the formation of hydrogen bonding between a base and a surface water molecule enabling the latter to make a nucleophilic attack to the silicon atom (Figure 1) [19-21]. This deteriorates the integrity of silica network and restricts its liquid applications to organic media or aqueous media at pH value less than 2 [19].

Recently we reported that the hydrolysis of SG could be significantly reduced by functionalizing its surface with a bulky aromatic group [21] or blocking the silanol groups with TiO_2 or ZrO_2 to break the unfavorable interaction between silica surface and medium [20,22]. However, these approaches are still beyond the wide applica-

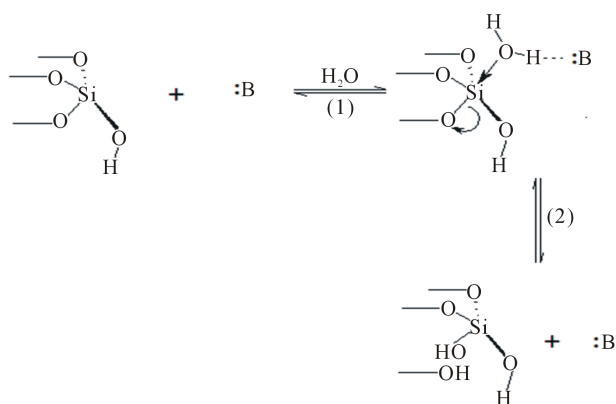


Figure 1. General base-catalyzed mechanism. :B is a general base.

tions of SG materials. On the other side, sol-gel chemistry can be used to provide the appropriate structural organization. The extraordinary opportunities offered by integrating solution chemistry of molecular entities with the solid-state nature of the gel provide the basis for designing a number of novel molecular materials [27-30]. The ease of solution based processing, choice of several precursors, and the ability to obtain the products in several different configurations and geometries are some of the appealing aspects of sol-gel-derived materials. The structural/functional modularity of SG allows a sequential modification of the parent material. In this fashion, through a judicious choice of dopants, new properties can be molecularly programmed in the sol-gels. Accordingly, the approach pursued in this work is based on doping F^- or Zr(IV) in a sol-gel-derived SG to yield useful new materials resistant to hydrolysis in aqueous media.

2. Experimental

2.1. Materials and Reagents

All reagents were of analytical grade A.R. and used without further purification. All solutions were prepared using Milli-Q water (MQW). SG chromatographic grade Kieselgel Geduran 60 (0.063 - 0.100 mm, BET surface area, $S_{\text{BET}} = 410 \text{ m}^2 \cdot \text{g}^{-1}$) was purchased from Merck (average particle size: 70 μm) and coded SGM. Sodium silicate solution (water glass) 36% SiO_2 was purchased from VWR-Germany. Stock 1000 $\text{mg} \cdot \text{L}^{-1}$ of Si (as Na_2SiO_3) and Zr (as ZrOCl_2) were used for the preparation of their standard solutions by appropriate dilution with MQW.

2.2. Apparatus

The analysis of Si and Zr was performed by a SPECTRO CIROS CCD Inductively Coupled Plasma-Optical Emission Spectrometer. The emission lines of Si at 212.412, 251.612 and 288.158 nm; Zr 257.139, 339.198 and 343.823 whereas the Ar lines at 404.442 and 430.01 nm were used to observe the stability of the generated plasma. IR transmittance spectra of the samples, prepared as a slurry in nujol, were recorded on a Bruker IFS 48 FTIR spectrometer. S_{BET} was determined with a Quantachrome Autosorb 1-MP using nitrogen at 77 K. Prior to the measurement, the samples were heated at 105°C in a vacuum for 12 h to remove surface contaminants and adsorbed water. S_{BET} was determined following the BET-Method [30] assuming a molecular cross section for N_2 of 16.2 \AA^2 . Pore size distributions were calculated by applying a NLDFT adsorption branch model assuming cylindrical pore geometry [31]. Powder X-ray diffractometry (XRD) was run on a Bruker D5000 system with $\text{Cu K}\alpha_1$ radiation (0.15406 nm) equipped with a graphite monochromator and scintillation counter from 14 to 84°2 θ , with step

width of $0.03^{\circ}2\theta$ and 7 seconds per step. Evaluation of the diffractograms was carried out with “Diffrac Plus EVA” version 13 by Bruker AXS. Raman spectra were recorded on a Bruker RAMII instrument. The pH of each sample solution was adjusted by NaOH and HCl solutions to be within the range (2 - 11) using an Orion pH/mV meter (model 330) and a combined Ross glass pH electrode (Orion 81-02) with Orion double junction Ag-AgCl reference electrode (model 90-02) containing 10% (w/v) potassium nitrate in the outer compartment.

2.3. Methodology

SG samples were synthesized by a sol-gel process. Sodium silicate solution (20 mL) was diluted to 200 mL H₂O and gradually acidified with concentrated HCl to pH 1. The formed gel was crushed and aged for 1 day. Then, the gel was washed with MQW to remove the formed NaCl and excess acid by decantation till pH > 5 then the dopant elements (Zr as ZrOCl₂·8H₂O, Merck or F⁻ as HF, 48%, Sigma-Aldrich) were added as solutions in 300 mL 1 mol·L⁻¹ HCl to the colloidal SG and thoroughly mixed for 4 h. Then the mixtures were dried in a drying oven at 90°C to get xero gel which was further dried at 200°C for 2 h then sintered at 500°C, 800°C and 1000°C for 6 h to develop sufficient mechanical stability of the resulting SG. The samples were quenched to room temperature in air, kept in closed bottles and coded as illustrated in **Table 1**.

In case of fluorination of SG from Merck, regarding that only 4 - 5 silanol groups per nm² of porous silica are accessible [1] and the S_{BET} of SG is 410 m²·g⁻¹, the accessible silanol groups for SG is calculated to be ≤ 3.41 mmol·g⁻¹. Consequently, the needed amount of F⁻ to replace silanol groups is 3.41 mmol·g⁻¹. This amount was used plus 25% extra amount to guarantee maximum surface covering. Hence, 5 g of SG was added to 20 mL distilled water in a polytetrafluoroethylene beaker at room temperature, then 0.9 mL HF was added and the suspension was shaken for 30 min, filtered, dried at 90°C over night and called FSGM.

The hydrolysis of SG phases in aqueous solution was investigated by adding 100 mg of the modified silica (grounded to <60 μm) to 200 mL of 0.1 mol·L⁻¹ HNO₃, MQW buffered by 0.5 mol·L⁻¹ NH₄Cl/NH₄OH to pH = 9.1 ± 0.1 and CH₃COOH/CH₃COONa to pH 4.5 ± 0.1 under continuous stirring. Aliquots of 6 mL were withdrawn with a syringe through a diaphragm membrane with a pore size of 0.20 μm type PET-20/25 from MACHEREY-NAGEL and hydrolyzed alkoxysilane was determined by inductively coupled plasma-optical emission spectrometry (ICP-OES).

3. Results and Discussion

Zr was chosen as dopants because: 1) Zirconia is tetra-

Table 1. Scheme of doping of silica gel.

Name	Sintering Temperature, °C	Dopant	Molar ratio of dopant to Si
FSG500	500	F	3/100
FSG800	800	F	3/100
FSG1000	1000	F	3/100
Zr1SG500	500	Zr	0.75/100
Zr1SG800	800	Zr	0.75/100
Zr1SG1000	1000	Zr	0.75/100
Zr2SG500	500	Zr	3.75/100
Zr2SG800	800	Zr	3.75/100
Zr2SG1000	1000	Zr	3.75/100
BSG500	500	-	-
BSG800	800	-	-
BSG1000	1000	-	-

valent that it may be easily incorporated in the silica matrix. 2) It is more electropositive than Si freeing partial negative charge to the Si-O bonding [20]. 3) Zr(IV) oxide is among the most stable oxides against hydrolysis [32]. Therefore, the nucleophilic attack on the silica surface is expected to be suppressed and the stability against hydrolysis improved. Fluorine was also used as dopant to decrease silica surface hydrolysis by the formation of the very stable Si-F bond [33].

3.1. XRD

Figure 2 shows the XRD patterns of the doped SG samples compared with the blank samples (BSG series) which are free of dopants. All samples show diffractograms of typical X-ray amorphous phases. Broad humps are observed at $2\theta = 21.53^{\circ} - 23.66^{\circ}$ in all samples, which are characteristic for the amorphous silica. Profile fitting of these peaks indicated that an increase in the d-spacing was observed as the sintering temperature increases (**Figure 3**). The largest d-spacing of the amorphous humps was observed for FSG1000 (4.098 Å) whilst the smallest d-spacing of them was observed for Zr2SG500 (3.895 Å).

The generalized β-cristobalite surface model for amorphous silica, suggested by Chuang and Maciel [34], may explain the observed increase in the d-spacing of the amorphous hump upon increasing the sintering temperature of the SG series. Despite the amorphous structure of SG means random stacking of SiO₄ tetrahedra, but the presence of that amorphous hump ((111)-like face) indicates the presence of a semi-ordered stacking of atoms in planes. The possible loss of structural water, upon heating, breaks the hydrogen bonding between the silanol groups of silica surfaces and consequently the gap between planes increases.

Doped SG samples heated at 500°C and 800°C show shorter d-spacing for the amorphous humps compared

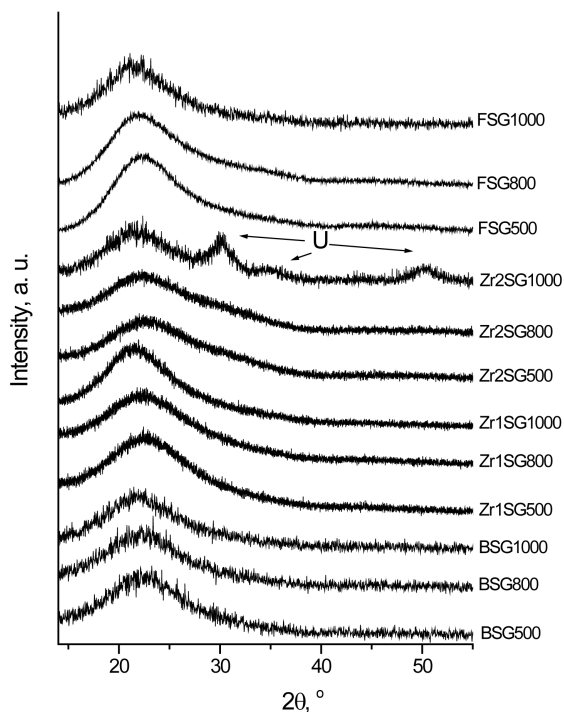


Figure 2. XRD patterns of doped SG samples. U = undetectable phase ($d = 2.95, 1.82, 1.55$).

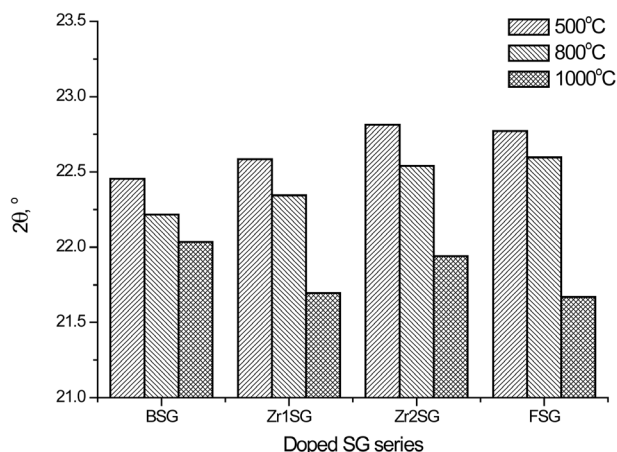


Figure 3. Effect of temperature on the 2θ values of the amorphous humps of doped SG samples.

with the pure samples whereas this behavior is reversed for the samples heated at 1000°C . This may indicate that the bonding between silica surface planes is improved in doped samples heated at 500°C and 800°C . Zr2SG1000 also shows XRD reflections from an unknown phase ($d = 2.95, 1.82$ and 1.55 \AA) which indicates a partial crystallization.

3.2. IR Spectra

IR spectra of BSG samples (Figure 4) showed absorption bands at $802 - 808, 972, 1000 - 1250$ (broad), $1630,$

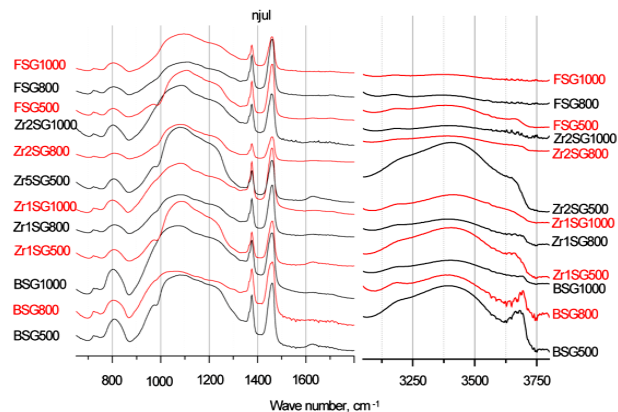


Figure 4. IR absorption spectra of doped SG samples.

$3170 - 3410$ (broad and multiple), $3663 - 3690 \text{ cm}^{-1}$ which are assignable to the vibration modes of Si-O-Si bending, Si-O-H stretching, Si-O-Si stretching, bending of molecular H_2O , hydrogen-bonded silanols stretching, and isolated silanols stretching, respectively [1]. The isolated silanol stretching band was observed to be red-shifted for the doped SG samples especially those doped with Zr and sintered at 500°C . This may indicate the reinforcement of Si-O bonding in case of Zr-doped samples via the more electropositive Zr freeing partial negative charge to the Si-O bonding. In case of F-doped samples, the powerful electron withdrawing experienced by the inductive effect of F, may similarly cause the reinforcement of Si-O bond.

Furthermore, the intensity of the bands due to OH vibration modes is observed to decrease as the sintering temperature increases especially in presence of dopants, that may be attributed to the loss of water as more silanol groups is transforming to siloxane, reversing Equation (1). This effect of temperature on amorphous silica is previously reported where an irreversible loss of water occurs at $T > 727^\circ\text{C}$ [35].

Moreover, IR spectra of the Zr-doped SG samples showed shoulders at $972 - 978 \text{ cm}^{-1}$, which are attributed to the stretching bands of the Si-O-Zr heterolinkage [36]. The stretching band for Si-OH group was superimposed onto the 972 cm^{-1} shoulder but it can be distinguished in the doped SG samples sintered at 1000°C , as the contribution from OH groups diminishes.

Other characteristic vibration bands, observed for the doped SG samples, are found comparable to those of BSG samples.

3.3. Raman Spectra

To confirm the presence of the Si-F bond in the F-doped SG samples, Raman spectra is elaborated. Also, the sample FSGM was synthesized by a simple room temperature treatment of SG from Merck with HF. Figure 5 presents the Raman spectra of the F-doped SG samples

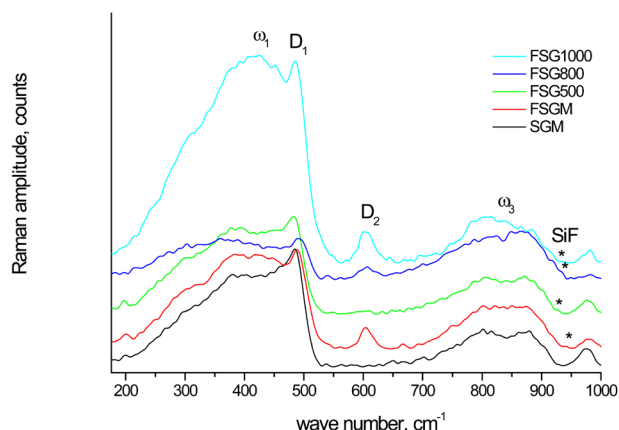


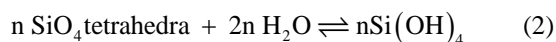
Figure 5. Raman spectra of fluorine-doped SG samples compared with SGM.

compared with SGM. The peaks at $930 - 970 \text{ cm}^{-1}$ (weak) are attributed to the Si-F stretching mode, whereas the spectral features at $380 - 440$ (broad peak), $480 - 490$ (sharp peak), 606 , and $800 - 875 \text{ cm}^{-1}$ are ascribable to the silica matrix and correspond to the ω_1 , D_1 , D_2 , and ω_3 modes, respectively [37]. The ω_n features arise from the band limits of the intrinsic phonon band structure of the tetrahedrally coordinated amorphous network of silicon dioxide [38], whereas D_1 and D_2 are attributed to the breathing modes of four and three membered planar rings of SiO_4 tetrahedra, respectively [39,40].

The presence of the Si-F peaks at $930 - 970 \text{ cm}^{-1}$ confirms the previous argument of the presence of Si-F bond in the F-doped SG samples. Moreover, the effect of the Si-F bond formation is observed to increase the degree of polymerization of the bulk SiO_4 tetrahedra as indicated from the increase in the D_2 feature of the FSGM compared with SGM. This phenomenon is also observed on raising the sintering temperature of FSG series due the condensation of the silanol groups.

3.4. Hydrolysis of Silica

The study of hydrolysis process is focused on the hydrolysis of the siloxane bond ($\equiv\text{SiOSi}\equiv$). When the silica surface is subjected to hydrolysis, which is the reverse reaction of the polymerization of silicic acid, variable oligomers of it are released from the SG matrix into solution according to the simplified reaction:



Hence, the hydrolysis process can be followed by measuring the hydrolyzed Si species. **Figure 6** shows the hydrolysis of the investigated SG samples during constant stirring for 60 min in MQW buffered at pH values 4.5, 9.1 and 9.1 using acetate, borate and ammonia buffers, respectively. **Table 2** summarizes the amounts of lost silica after 60 min of stirring of SG samples in the

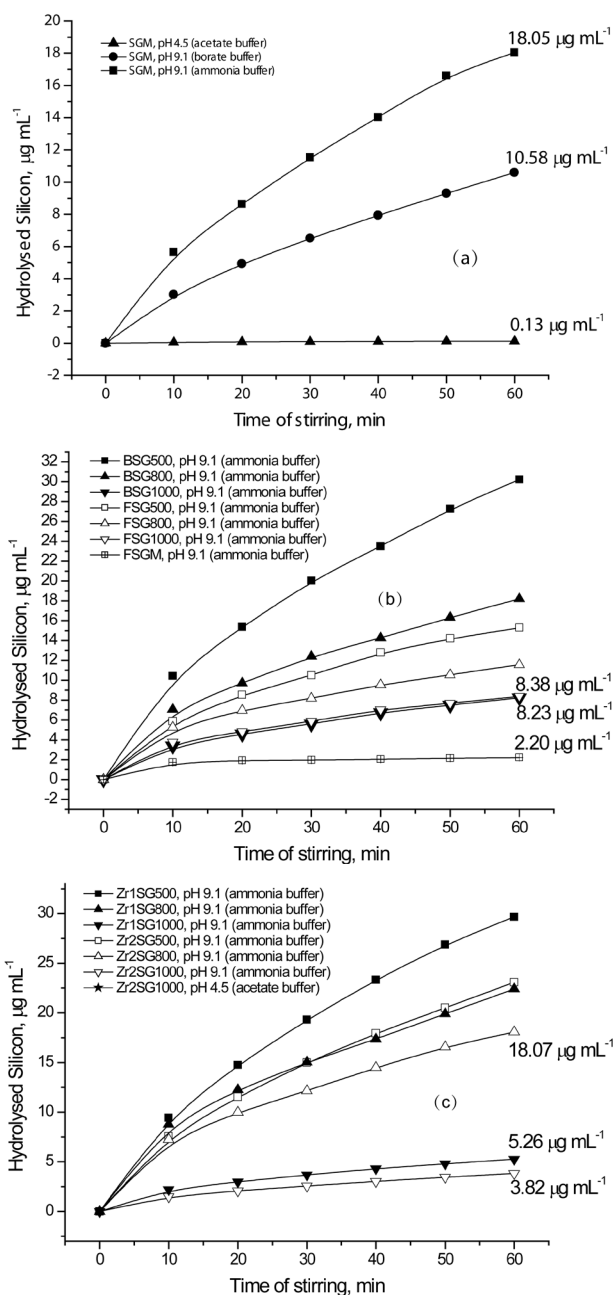


Figure 6. Effect of pH, type of buffer and dopant on the hydrolysis of silica.

buffered solutions

Higher Si concentration means more hydrolysis and less stability of silica. Accordingly, more silica hydrolysis is observed in weak basic medium than in weak acidic medium (**Figure 6(a)** and **Table 2**). Nevertheless, ammonia buffer enhances hydrolysis ca. twice as borate buffer does despite they have the same pH value ($[\text{OH}^-] 1.26 \times 10^{-5} \text{ mol}\cdot\text{l}^{-1}$). So, ammonia buffer is chosen in the next hydrolysis studies to explore the effect of surface area of SG and the presence of a dopant on the hydrolysis process.

Table 2. Hydrolysed silica (%) from 0.1 g SG in 200 mL of the buffer solution under constant stirring for 60 min, calculated from the measured Si concentration.

Name	Buffer solution (pH)	Hydrolyzed SiO ₂ (%)
SGM	Acetate (4.5)	0.05
SGM	Borate (4.5)	3.86
SGM	Ammonia (9.1)	6.58
FSGM	Ammonia (9.1)	0.80
FSG500	Ammonia (9.1)	5.57
FSG800	Ammonia (9.1)	4.22
FSG1000	Ammonia (9.1)	3.05
Zr1SG500	Ammonia (9.1)	10.81
Zr1SG800	Ammonia (9.1)	8.16
Zr1SG1000	Ammonia (9.1)	1.92
Zr2SG500	Ammonia (9.1)	8.41
Zr2SG800	Ammonia (9.1)	6.58
Zr2SG1000	Ammonia (9.1)	1.39
BSG500	Ammonia (9.1)	11.00
BSG800	Ammonia (9.1)	6.64
BSG1000	Ammonia (9.1)	3.00

Regarding the effect of sintering temperature on silica hydrolysis at pH 9.1 using ammonia buffer (Figure 6(b), (c) and Table 2), all SG samples show direct proportion- al relationship. The order of stability of SG against hydrolysis is 1000°C > 800°C > 500°C. The doped samples obviously show better resistivity to hydrolysis when compared with BSG series except for FSG1000. The high resistivity of FSGM towards hydrolysis indicates the effect of the replacement of silanols by Si-F losing the hydrophobic character of silica. It is worth mentioning that, the difference in hydrolysis (%) between BSG and FSG series decreases as the sintering temperature increases. On the other hand, the silica hydrolysis is observed to increase in the order Zr2SG < Zr1SG < BSG, which indicates the inhibition effect of Zr(IV) on the hydrolysis process of silica. It is noteworthy to state that, the difference in hydrolysis (%) between BSG and Zr-SG series increases as the sintering temperature increases. This may be attributed to the better occlusion of Zr(IV) in the silica network with increasing the sintering temperature.

Despite the observed success in inhibiting hydrolysis of silica by doping SG with Zr(IV) or F, an important factor should be addressed which is the surface area (S_{BET}), as far as the hydrolysis process is a surface phenomenon. Hence, S_{BET} and the porosities of selected SG samples at different sintering temperatures were studied (Table 3). The S_{BET} values are from 181.5 to 570 m²/g and all samples undergo mesoporous structures as observed from the unimodal distribution of mesoporous structure that obtained from pore volume distribution

Table 3. Surface area parameters of selected SG samples.

Sample	S _{BET} m ² /g	Pore volume distribution				Average pore width nm
		Total	Macro	Meso	Micro	
BSG800	524	0.535	-	0.535	0	5.7
BSG1000	273	0.246	-	0.246	0	4.9
Zr1SG1000	240	0.246	0.001	0.241	0.004	6.1
Zr2SG800	481	0.534	0.001	0.533	0	5.9
Zr2SG1000	182	0.187	-	0.186	0.0012	5.9
FSG800	266	0.689	-	0.689	-	13.9
FSG1000	190	0.618	0.002	0.617	0	11.7
FSGM	73	0.689	-	0.689	0	13.0

analysis (Figure 7). The S_{BET}, total pore volume and average pore width values decrease as the temperature increases especially at 1000°C due to the condensation of silanol groups as supposed from the results of XRD and IR. Doping with Zr(IV) or F⁻ decrease S_{BET} values compared with the BSG that may explain the decrease in silica hydrolysis. Nevertheless, F is observed to enlarge the average pore width remarkably. The contraction in S_{BET} of SG from 410 m²·g⁻¹ to 72.9 m²·g⁻¹ in FSGM and the relatively large average pore width of FSGM (13.0 nm) may be due to the corrosive effect of HF leading to the formation of wider pores.

To understand the effect of dopant, free from the effect of surface area, a function (*H*) was suggested to represent the so called “specific hydrolysis”. *H* is obtained by dividing the rate of hydrolysis (μg·mL⁻¹·min⁻¹·g⁻¹, denoted by *r*) by S_{BET} (m²·g⁻¹), considering the hydrolysis process is a SN₂ reaction and assuming that the surface population of siloxane groups per square meter is constant in the studied samples, using Equation (3).

$$H = \frac{r}{S_{\text{BET}}} \quad (3)$$

The effect of dopant *H* is tabulated in Table 4. The specific hydrolysis increases in the order FSGM < Zr1SG1000 < Zr2SG1000 < BSG1000 < BSG800 < Zr2SG800 < FSG800 < FSG1000 < SGM. Obviously, the stability of silica is improved by increasing the sintering temperature due to that the surface becomes less hydrophilic attributed to the condensation of silanol groups as confirmed by IR. Accordingly, the room temperature-fluorinated SGM (FSGM) is the most stable silica against hydrolysis due to the partial replacement of the powerful Si-F with the surface silanol groups. In addition, this may decrease the hydrophilic properties of the silica surface and consequently leads to smaller diffusion of corrosive ions. Similar hydrophobic behavior was reported elsewhere for organically-modified silica [21,41]. Also, the inductive effect of fluoride groups was reported to enhance the reactivity of the residual silanol groups

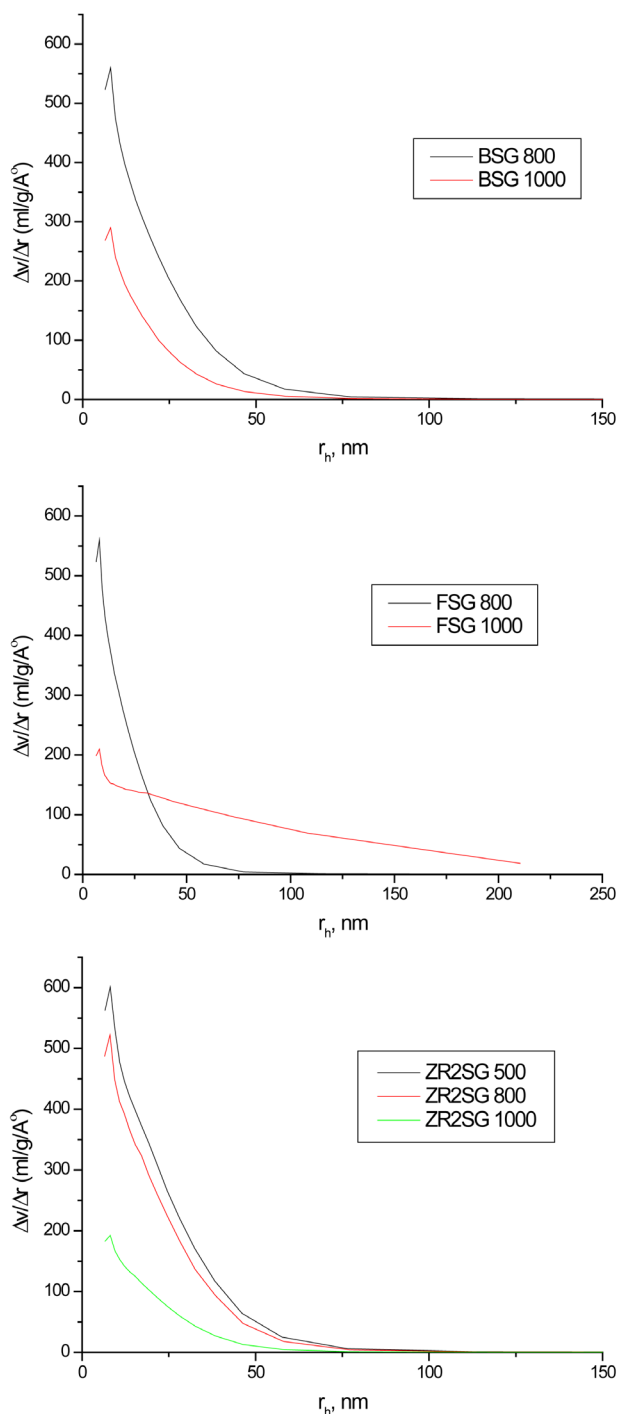


Figure 7. Representative pore volume distribution of FSG500, FSG1000, Zr2SG500 and Zr2SG1000.

[42]. In contrary, bulk doping of silica with fluoride group, slightly increases the silica hydrolysis probably due to the easier ion diffusion in the relatively large pores of FSG series.

Moreover, Zr1SG1000 and Zr2SG1000 show better stability compared with BSG1000 which may be attributed to that Zr is more electropositive than Si making it

Table 4. Effect of sample type on the silica hydrolysis.

Material	S_{BET} , $m^2 \cdot g^{-1}$	r ($\mu g \cdot mL^{-1} \cdot min^{-1} \cdot g^{-1}$)	H ($\mu g \cdot mL^{-1} \cdot min^{-1} \cdot m^2 \times 10^3$)
BSG1000	273	0.97	3.56
BSG800	524	2.22	4.23
Zr1SG1000	240	0.61	2.56
Zr2SG1000	182	0.46	2.56
Zr2SG800	481	2.18	4.54
FSG800	266	1.25	4.72
FSG1000	190	0.94	4.94
FSGM	73	0.09	1.25
SGM	410 ^a	2.52	6.15

^aThe value of S_{BET} is taken from the labelled parameters of the manufacturer.

more resisting to SN_2 reaction. These results are in agreement with those obtained from the covering of SG and organically-modified SG with zirconia [20,22]. The well occlusion of Zr in the amorphous silica network at 1000°C, which is confirmed by the absence of Zr phases in their XRD diffractograms and the appearance of IR absorption bands of the Zr-O-Si heterolinkage, may be additional reason for the stability of samples sintered at 1000°C compared with those sintered at 800°C.

4. Conclusions

The hydrolysis of silica gel is SN_2 reaction affected by the pH of solution, the type of the nucleophilic base, sintering temperature, surface area and the presence of a dopant. The hydrolysis process increases as the pH value of solution increases. Ammonia catalyzes hydrolysis more than hydroxide causing disintegration of the 3D silica network. The stability of silica increases as sintering temperature increases due to the decrease of the surface area of the silica and the condensation of silanol groups.

Fluorination of SG surface with HF may be an effective room temperature method to decrease silica hydrolysis but this has the disadvantage of lowering the hydrophilic nature of silica as well as its surface area. The reason of this effect is the formation of the most stable and the less hydrophilic SiF groups instead of SiOH groups. Moreover, the inductive effect of fluoride group may suppress the SN_2 attack to Si(IV). Bulk F-doping of SG slightly increases hydrolysis probably due to the formation of wider pores and better diffusibility of FSG.

Furthermore, Zr(IV) is observed to be an effective bulk-dopant to lower silica hydrolysis while maintaining its large surface area and hydrophilic nature. This is explained by the relative higher electropositivity of Zr compared with Si, which may decrease the SN_2 attack to Si(IV).

Acknowledgements

This work has been partly funded by the Alexander von Humboldt foundation, Germany, in the frame of a fellowship award.

REFERENCES

- [1] R. K. Iler, "The Chemistry of Silica," Wiley, New York, 1979.
- [2] E. F. Vansant, P. Van der Voort and K. C. Vrancken, "Characterisation and Chemical Modification of the Silica Surface," Elsevier, Amsterdam, 1995.
- [3] J. Andersson, S. Areva, B. Spliethoff and M. Lindén, "Sol-Gel Synthesis of a Multifunctional, Hierarchically Porous Silica/Apatite Composite," *Biomaterials*, Vol. 26, No. 34, 2005, pp. 6827-6835.
<http://dx.doi.org/10.1016/j.biomaterials.2005.05.002>
- [4] H. J. Erli, R. Marx, O. Paar, F. U. Niethard, M. Weber and D. C. Wirtz, "Surface Pretreatments for Medical Application of Adhesion," *BioMedical Engineering OnLine*, Vol. 2, 2003, p. 15.
- [5] E. M. Claesson, N. C. Mehendale, R. J. M. K. Gebbink, G. van Kotenb and A. P. Philipse, "Magnetic Silica Colloids for Catalysis," *Journal of Magnetism and Magnetic Materials*, Vol. 311, 2007, pp. 41-45.
<http://dx.doi.org/10.1016/j.jmmm.2006.11.166>
- [6] S. Antebi, P. Arya, L. E. Manzer and H. Alper, "Carbonylation Reactions of Iodoarenes with PAMAM Dendrimer-Palladium Catalysts Immobilized on Silica," *The Journal of Organic Chemistry*, Vol. 67, No. 19, 2002, pp. 6623-6631. <http://dx.doi.org/10.1021/jo020271n>
- [7] S. C. Bourque, F. Maltais, W.-J. Xiao, O. Tardif, H. Alper, P. Arya and L. E. Manzer, "Hydroformylation Reactions with Rhodium-Complexed Dendrimers on Silica," *Journal of the American Chemical Society*, Vol. 121, No. 13, 1999, pp. 3035-3038.
<http://dx.doi.org/10.1021/ja983764b>
- [8] J. Kurczewska and G. Schroeder, "Modified Silica Surface by Phenylboronic Acid Derivatives as Effective Sugar Sensor," *Central European Journal of Chemistry*, Vol. 7, No. 4, 2009, pp. 697-701.
<http://dx.doi.org/10.2478/s11532-009-0080-5>
- [9] M. R. J. Rui, R. L. Phabyanno, G. C. Alessandra, S. R. Adriana, C. De Abreu Fabiane, O. F. G. Marilia and T. K. Lauro, "An Amperometric Sensor Based on Hemin Adsorbed on Silica Gel Modified with Titanium Oxide for Electrocatalytic Reduction and Quantification of Artemisinin," *Talanta*, Vol. 77, No. 2, 2008, pp. 909-914.
- [10] J. D. S. Newman, J. M. Roberts and G. J. Blanchard, "Optical Organophosphate Sensor Based upon Gold Nanoparticle Functionalized Fumed Silica Gel," *Analytical Chemistry*, Vol. 79, No. 9, 2007, pp. 3448-3454.
<http://dx.doi.org/10.1021/ac062165h>
- [11] C.-Y. Yen, C.-H. Lee, Y.-F. Lin, H.-L. Lin, Y.-H. Hsiao, S.-H. Liao, C.-Y. Chuang and C.-C. M. Ma, "Sol-Gel Derived Sulfonated-Silica/Nafion® Composite Membrane for Direct Methanol Fuel Cell," *Journal of Power Sources*, Vol. 173, No. 1, 2007, pp. 36-44.
<http://dx.doi.org/10.1016/j.jpowsour.2007.08.017>
- [12] Y.-F. Lin, C.-Y. Yen, C.-C. M. Ma, S.-H. Liao, C.-H. Lee, Y.-H. Hsiao and H.-P. Lin, "High Proton-Conducting Nafion®/–SO₃H Functionalized Mesoporous Silica Composite Membranes," *Journal of Power Sources*, Vol. 171, No. 2, 2007, pp. 388-395.
<http://dx.doi.org/10.1016/j.jpowsour.2007.06.049>
- [13] D. Gomes, I. Buder and S. P. Nunes, "Sulfonated Silica-Based Electrolyte Nanocomposite Membranes," *Journal of Polymer Science Part B: Polymer Physics*, Vol. 44, No. 16, 2006, pp. 2278-2298.
<http://dx.doi.org/10.1002/polb.20868>
- [14] Kh. Abou-El-Sherbini, M. Hassanien and I. Kenawy, "Selective Separation and Preconcentration of Total Tin Using Quercetin as Chelating Agent," *Separation Science and Technology*, Vol. 42, No. 15, 2007, pp. 3447-3463.
<http://dx.doi.org/10.1080/01496390701653911>
- [15] M. Hassanien and Kh. Abou-El-Sherbini, "Synthesis and Characterisation of Morin-Functionalised Silica Gel for the Enrichment of Some Precious Metal Ions," *Talanta*, Vol. 68, No. 5, 2006, pp. 1550-1559.
<http://dx.doi.org/10.1016/j.talanta.2005.08.016>
- [16] G. Mostafa, M. Hassanien, Kh. Abou-El-Sherbini and V. Görlitz, "Controlled-pore Silica Glass Modified with N-Propylsalicylaldimine for the Separation and Preconcentration of Trace Al(III), Ag(I) and Hg(II) in Water Samples," *Analytical Sciences*, Vol. 19, No. 8, 2003, pp. 1151-1156. <http://dx.doi.org/10.2116/analsci.19.1151>
- [17] P. K. Jal, S. Patel and B. K. Mishra, "Chemical Modification of Silica Surface by Immobilization of Functional Groups for Extractive Concentration of Metal Ions," *Talanta*, Vol. 62, No. 5, 2004, pp. 1005-1028.
<http://dx.doi.org/10.1016/j.talanta.2003.10.028>
- [18] F. Barbette, F. Rascalou, H. Chollet, J. L. Babouhot, F. Denat and R. Guillard, "Extraction of Uranyl Ions from Aqueous Solutions Using Silica-Gel-Bound Macrocycles for Alpha Contaminated Waste Water Treatment," *Analytica Chimica Acta*, Vol. 502, No. 2, 2004, pp. 179-187.
<http://dx.doi.org/10.1016/j.aca.2003.09.065>
- [19] M. Etienne and A. Walcarius, "Analytical Investigation of the Chemical Reactivity and Stability of Aminopropyl-Grafted Silica in Aqueous Medium," *Talanta*, Vol. 59, No. 6, 2003, pp. 1173-1185.
[http://dx.doi.org/10.1016/S0039-9140\(03\)00024-9](http://dx.doi.org/10.1016/S0039-9140(03)00024-9)
- [20] Kh. Abou-El-Sherbini, C. Pape, O. Rienitz, D. Schiel, R. Stosch, P. G. Weidler, W. H. Höll, "Stabilization of *n*-Aminopropyl Silica Gel against Hydrolysis by Blocking Silanol Groups with TiO₂ or ZrO₂," *Journal of Sol-Gel Science and Technology*, Vol. 53, No. 3, 2010, pp. 587-597. <http://dx.doi.org/10.1007/s10971-009-2136-6>
- [21] Kh. Abou-El-Sherbini, "Modification of Aminopropyl Silica Gel with Some Chelating Agents and Their Effect on Its Stability against Hydrolysis," *Journal of Sol-Gel Science and Technology*, Vol. 51, No. 2, 2009, pp. 228-237. <http://dx.doi.org/10.1007/s10971-009-1975-5>
- [22] Kh. Abou-El-Sherbini, D. Schiel, R. Stosch, P. G. Weidler and W. H. Höll, "Stabilization of Quercetin—Functionalized Silica Gel against Hydrolysis by Blocking Silanol Groups with TiO₂ or ZrO₂ and Its Application for

- the Removal of Hg(II),” *Journal of Sol-Gel Science and Technology*, Vol. 57, No. 1, 2010, pp. 57-67.
- [23] R. Dron, F. Brivot and T. Chaussadent, “Mechanism of the Alkali-Silica Reactions,” *10th International Conference on the Chemistry of Cement*, Gothenburg, Vol. 4, 1997, 4iv074-8p.
- [24] B. V. Zhmud and J. Sonnefeld, “Aminopolysiloxane Gels: Production and Properties,” *Journal of Non-Crystalline Solids*, Vol. 195, No. 1-2, 1996, pp. 16-27. [http://dx.doi.org/10.1016/0022-3093\(95\)00497-1](http://dx.doi.org/10.1016/0022-3093(95)00497-1)
- [25] A. A. Golub, A. I. Zubenko and B. V. Zhmud, “ γ -APTES Modified Silica Gels: The Structure of the Surface Layer,” *Journal of Colloid and Interface Science*, Vol. 179, No. 2, 1996, pp. 482-487. <http://dx.doi.org/10.1006/jcis.1996.0241>
- [26] B. V. Zhmud and A. B. Pechenyi, “Acid-Base Properties and Electrokinetic Behavior of Amine-Containing Organopolysiloxane Matrices,” *Journal of Colloid and Interface Science*, Vol. 173, No. 1, 1995, pp. 71-78. <http://dx.doi.org/10.1006/jcis.1995.1298>
- [27] A. Rimola, D. Costa, M. Sodupe, J.-F. Lambert and P. Ugliengo, “Silica Surface Features and Their Role in the Adsorption of Biomolecules: Computational Modeling and Experiments,” *Chemical Reviews*, Vol. 113, No. 6, 2013, pp. 4216-4313. <http://dx.doi.org/10.1021/cr3003054>
- [28] B. C. Dave and E. A. J. Ottosson, “Sol-Gel Encapsulation of Molecules to Generate Functional Optical Materials: A Molecular Programming Approach,” *Journal of Sol-Gel Science and Technology*, Vol. 31, No. 1-3, 2004, 303-307. <http://dx.doi.org/10.1023/B:JSSST.0000048008.73055.22>
- [29] Y. Y. Han and D. Zhang, “Ordered Mesoporous Silica Materials with Complicated Structures,” *Current Opinion in Chemical Engineering*, Vol. 1, No. 2, 2012, pp. 129-137. <http://dx.doi.org/10.1016/j.coche.2011.11.001>
- [30] S. Brunauer, P. H. Emmett and E. Teller, “Adsorption of Gases in Multimolecular Layers,” *Journal of the American Chemistry Society*, Vol. 60, No. 2, 1938, pp. 309-319. <http://dx.doi.org/10.1021/ja01269a023>
- [31] M. Thommes, “Chapter 11: Physical Adsorption Characterization of Ordered and Amorphous Mesoporous Materials,” In: G. Q. Lu and X. S. Zhao, Eds., *Nanoporous Materials: Science and Engineering*, Imperial College Press, London, 2004, pp. 317-364.
- [32] J. Ryan, M. Elimelech, J. Baeseman and R. Magelky, “Silica-Coated Titania and Zirconia Colloids for Sub-surface Transport Field Experiments,” *Environmental Science & Technology*, Vol. 34, No. 10, 2000, pp. 2000-2005. <http://dx.doi.org/10.1021/es9909531>
- [33] G. F. Cerofolini, “A Study of the Ionic Route for Hydrogen Terminations Resulting after SiO₂ Etching by Concentrated Aqueous Solutions of HF,” *Applied Surface Science*, Vol. 133, No. 1-2, 1998, pp. 108-114. [http://dx.doi.org/10.1016/S0169-4332\(98\)00182-2](http://dx.doi.org/10.1016/S0169-4332(98)00182-2)
- [34] I. S. Chuang and G. E. Maciel, “A Detailed Model of Local Structure and Silanol Hydrogen Bonding of Silica Gel Surfaces,” *The Journal of Physical Chemistry B*, Vol. 101, No. 16, 1997, pp. 3052-3064. <http://dx.doi.org/10.1021/jp9629046>
- [35] B. A. Morrow, I. A. Cody and L. S. M. Lee, “Infrared Studies of Reactions on Oxide Surfaces. 7. Mechanism of the Adsorption of Water and Ammonia on Dehydroxylated Silica,” *The Journal of Physical Chemistry*, Vol. 80, No. 25, 1976, pp. 2761-2767. <http://dx.doi.org/10.1021/j100566a009>
- [36] S. W. Lee and R. A. Condrate, “The Infrared and Raman Spectra of ZrO₂-SiO₂ Glasses Prepared by a Sol-Gel Process,” *Journal of Materials Science*, Vol. 23, No. 8, 1988, pp. 2951-2959. <http://dx.doi.org/10.1007/BF00547474>
- [37] R. Lorenzi, S. Brovelli, F. Meinardi, A. Lauria, N. Chiodini and A. Paleari, “Role of Sol-Gel Networking and Fluorine Doping in the Silica Urbach Energy,” *Journal of Non-Crystalline Solids*, Vol. 357, No. 8-9, 2011, pp. 1838-1841. <http://dx.doi.org/10.1016/j.jnoncrysol.2010.12.051>
- [38] F. L. Galeener, “Band Limits and the Vibrational Spectra of Tetrahedral Glasses,” *Physical Review B*, Vol. 19, No. 8, 1979, pp. 4292-4297. <http://dx.doi.org/10.1103/PhysRevB.19.4292>
- [39] F. L. Galeener, “Planar Rings in Glasses,” *Solid State Communications*, Vol. 44, No. 7, 1982, pp. 1037-1040. [http://dx.doi.org/10.1016/0038-1098\(82\)90329-5](http://dx.doi.org/10.1016/0038-1098(82)90329-5)
- [40] A. Pasquarello and R. Car, “Identification of Raman Defect Lines as Signatures of Ring Structures in Vitreous Silica,” *Physical Review Letters*, Vol. 80, No. 23, 1998, pp. 5145-5147. <http://dx.doi.org/10.1103/PhysRevLett.80.5145>
- [41] Y. Sohrin, S. Iwamoto, S. Akiyama, T. Fujita, T. Kugii, H. Obata, E. Nakayama, S. Goda, Y. Fujishima, H. Hasegawa, K. Ueda and M. Matsui, “Determination of Trace Elements in Seawater by Fluorinated Metal Alkoxide Glass-Immobilized 8-Hydroxyquinoline Concentration and High-Resolution Inductively Coupled Plasma Mass Spectrometry Detection,” *Analytica Chimica Acta*, Vol. 363, No. 11, 1998, pp. 11-19. [http://dx.doi.org/10.1016/S0003-2670\(98\)00074-9](http://dx.doi.org/10.1016/S0003-2670(98)00074-9)
- [42] G. F. Cerofolini and N. Re, In: E. Garfunkel, E. Gusev and Y. A. Vul’, *Fundamental Aspects of Ultra Thin Dielectric on Si-Based Devices*, Kluwer, Dordrecht, 1998.